

Two-Step Disordering of Perpendicularly Magnetized Ultrathin Films

A. Vaterlaus,¹ C. Stamm,¹ U. Maier,¹ M. G. Pini,² P. Politi,³ and D. Pescia¹

¹Laboratorium für Festkörperphysik, Eidgenössische Technische Hochschule Zürich, CH-8093 Zürich, Switzerland

²Istituto di Elettronica Quantistica, CNR, Via Panciatichi 56/30, I-50127 Firenze, Italy

³INFN, Unita di Firenze, Largo Enrico Fermi 2, I-50127 Firenze and Fachbereich Physik, Universität GH Essen, D-45117 Essen, Germany

(Received 1 September 1999)

We have imaged the stripe domain structure of perpendicularly magnetized fcc ultrathin Fe films grown on Cu(100). The stripe phase has a strong local orientational order and sustains the two kinds of fluctuations predicted by Abanov *et al.* [Phys. Rev. B **51**, 1023 (1995)]: meandering and dislocations. Before reaching the Curie temperature, the stripes transform into a new and so far unobserved domain structure, characterized by domains with predominantly square corners. We argue that this phase is the tetragonal liquid phase proposed by Abanov *et al.* to separate the stripe phase from the paramagnetic phase. This two-step disordering is reminiscent of a two-dimensional melting process.

PACS numbers: 75.70.Kw, 05.70.Fh, 75.40.-s

Micrometer thick films, magnetized perpendicular to the film plane, typically break into stripes consisting of spins aligned “up” and “down” [1–4]. The formation of the stripe phase is the result of the competition between the exchange interaction—favoring parallel alignment of neighboring spins—and the much weaker but long ranged dipolar coupling, which favors antiparallel alignment over large distances [1,2]. Application of a magnetic field transforms the stripes into a variety of complex domain patterns, including undulation, chevrons, bubble, and labyrinthine patterns, with fork and dead-end-type defects [3,4]. It was suggested that these complex patterns “follow the analogous *three-dimensional* scenario encountered with smectic liquid crystals” [4].

In a landmark paper by Yafet and Gyorgy [5] (see also Ref. [6,7]), the stripe phase was proposed as the ground state of the perpendicularly magnetized *monolayer* in the zero applied magnetic field. Such stripes were indeed found in ultrathin, 2–3 AL thick (AL: atomic layer), magnetic films of fcc Fe on Cu(100) [8]. Czech and Villain [6] proposed that, at finite temperatures and in zero applied magnetic field, the stripe phase in the monolayer forms a two-dimensional “floating” solid, of the type discussed by Nelson and Halperin [9–11]. A floating stripe phase consists of orientationally ordered stripes that have infinitely large position fluctuations [10,11]. In 1995, Abanov *et al.* [12] worked out some properties of the floating phase. They proposed that (i) the orientational order is perturbed by (ii) two classes of fluctuations: “meandering,” i.e., undulations of the stripes around the preferential orientation, and four types of topological defects, i.e., defects localized in space; see the inset in Fig. 2A. They suggested further that, before reaching the paramagnetic state, (iii) the stripe phase transforms into an intermediate state, characterized by domains with predominantly square corners. The square corners are imposed by the square symmetry of the fcc lattice, which provides two mutually orthogonal equivalent directions. They called this interme-

diated phase “tetragonal liquid.” Monte Carlo simulations by Booth *et al.* [13] have produced a real space picture of this phase, which we will use for comparison with our experiments. The novel element introduced in Ref. [12] is the two-step character of the disordering in zero applied magnetic field. This feature, which is apparently absent in micrometer thick magnetic films [2–4], is reminiscent of a two-dimensional melting process [11,14].

In this paper, we have imaged the stripe phase of atomically thin magnetic films of fcc Fe on Cu(100) as it evolves with temperature and in zero applied magnetic field. We provide experimental observations of the predicted features (i)–(iii). To our knowledge, meandering has been already observed in thick films, while a systematic observation of the four types of topological defects has not been reported yet. The tetragonal liquid domain structure was observed here for the first time. We measure the spatial distribution of the magnetization vector using SEMPA (scanning electron microscopy with polarization analysis) [8,15]. In this technique, the spin polarization vector of the electrons excited out of the top ≈ 5 surface layers by a focused electron beam of diameter ≈ 20 nm is detected and is a measure of the magnetization vector within the beam focus. We studied ultrathin extended fcc Fe films (by extended we mean with lateral size of the order of mm) of thickness less than 5 AL. All the films are grown at room temperature. Thus, the films are either paramagnetic or perpendicularly magnetized, depending on their temperature and thickness, in agreement with previous studies [16–18]. In all the images, only the perpendicular component is shown, which is the only nonzero one. The grey scale is proportional to this component, “white” and “black” corresponding to regions of up and down magnetization, respectively. The thickness of the extended films is determined by Auger spectroscopy with an accuracy of $\pm 20\%$ [19].

Figure 1A shows the local magnetization for a film in the stripe phase. The stripes show a pronounced meandering—one type of fluctuation predicted by theory

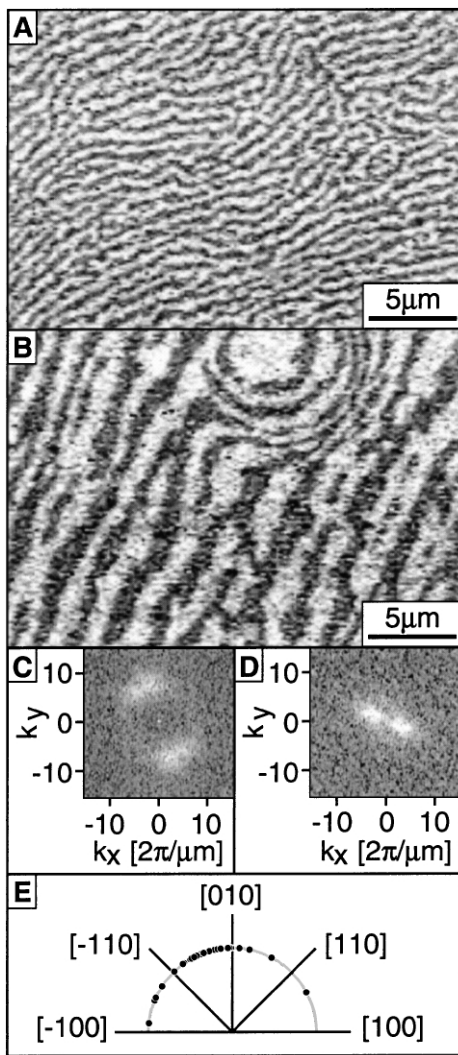


FIG. 1. Stripe phase in ultrathin films, at room temperature. The films in (A) and (B) are 2.6 ± 0.6 AL thick. The vertical direction is the [010]. (C) and (D) show the two-dimensional Fourier power spectrum of (A) and (B), respectively. (E) is a polar plot summarizing the propagation directions observed in many images.

[12]—but have local orientational order (“local” means extending over $20\text{--}40\ \mu\text{m}$ typically); i.e., they form a two-dimensional plane wave propagating in a well-defined planar direction. The existence of a preferred orientation is rendered explicit in Fig. 1C. This figure plots the square of the Fourier coefficients obtained by Fourier transforming Fig. 1A (the so-called Fourier power spectrum). The grey scale is proportional to the strength of these coefficients: thus, whiter regions locate those plane waves which are more prominent in the Fourier transform of Fig. 1A. As shown in Fig. 1C, the stripes form a wave predominantly propagating in one direction. Figure 1B shows a different film as in Fig. 1A, Fig. 1D being the corresponding Fourier power spectrum. The local propagation direction has changed slightly. Figure 1E plots a polar summary of the mean propagation directions (black dots), deter-

mined from the Fourier power spectrum of many images of the same sample and of different samples. The data of Fig. 1E support the existence of a globally preferred propagation direction which concentrates between the $[-110]$ and the $[010]$ in-plane directions of the fcc lattice. Long range orientational order should indeed appear in a floating solid [10,12].

Besides meandering excitations, the stripe phase contains topological excitations; see Fig. 2A. The inset of this figure summarizes the topological defects predicted to occur in the monolayer; see Fig. 2 in Ref. [12]. We systematically observe the occurrence of these four types of defects, marked by arrows in Fig. 2A and labeled with a , b , c , and d . Occasionally, we observed “circular” (Figs. 1B and 2B) defects. In these defects, the stripes of up and down spins are arranged as concentric rings. We refrain from calling these defects “vortices,” a name that seems to be reserved for a situation where the *spins* rotate in a vortexlike manner [20]. At present, we are not aware of any paper predicting these defects in the monolayer, although defects with stripes winding around a central part resemble the labyrinthine configuration that develops in thicker films. Occasionally, the stripes organize themselves into chevronlike defects; see Fig. 2C. Again, we are not aware of any theoretical work predicting these defects in the monolayer, although they are very common in thick films [3,4]. Notice that topographic images

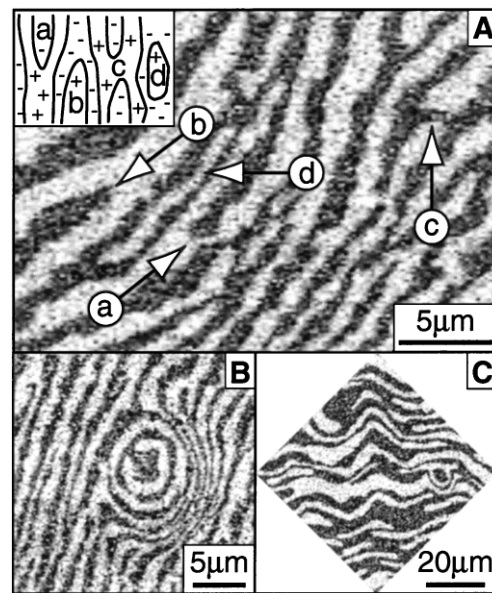


FIG. 2. Topological fluctuations in ultrathin films. Thickness: 2.6 ± 0.6 AL. Vertical direction: [010]. (A). In the inset, the four classes of topological defects described in Ref. [12] are sketched. (a) The dislocation, region of down spins (indicated with $-$), is inserted from above. (b) Dislocation inserted from below. (c) “passage” due to two dislocations, one inserted from above and one inserted from below. (d) “island,” due to two dislocations inserted in the center, one ending above and one ending below the center. (B) Circularlike defect. (C) chevronlike defects.

(taken with the SEMPA simultaneously to the magnetization image) do not reveal any particular morphological defect at the location of these magnetic singularities.

In order to study the evolution of the striped phase when the film is brought closer to the magnetic-paramagnetic phase transition, we grow a wedgelike Fe film [15]. As suggested by previous studies of the phase transition of fcc Fe films grown at room temperature [16–18,21], the Curie temperature of films thinner than ≈ 2 AL and thicker than ≈ 5 AL is less than room temperature, exceeding room temperature only for intermediate thicknesses. Accordingly, the magnetic image of a wedgelike film taken at room temperature (Fig. 3A) reveals a window of nonzero perpendicular magnetization with a stripe phase similar to the one described in Figs. 1 and 2. Outside this window we observe a “grey” region with zero polarization (we will discuss this region, which we tentatively call “paramagnetic,” later in the paper). In Fig. 3A, the thickness of the Fe film increases from 1.6 AL (right-hand side) to 4 AL (left-hand side). Images of the edges of the window are representative for films closer to T_C than the images at the center of the window. Thus, by moving from the center of the window toward its edges, one can observe the film disordering at a fixed temperature.

Figure 3A reveals one important characteristic of the disordering process: the width of the stripes reduces when the paramagnetic phase is approached, as predicted and

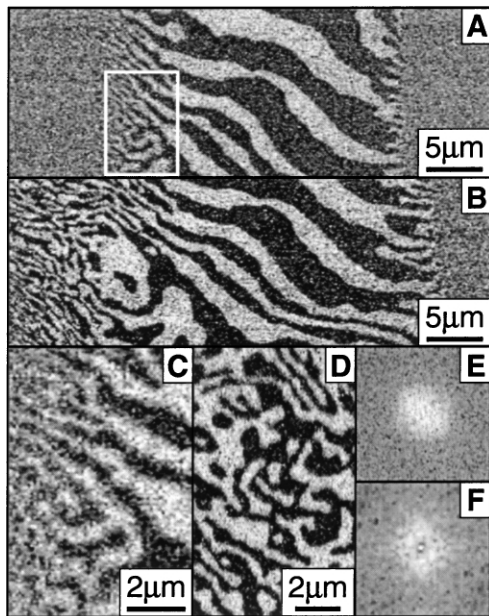


FIG. 3. Orientational melting. The vertical direction is $[-110]$. (A) Section of a magnetically active window at room temperature. The film thickness increases from 1.6 AL (right-hand side) to 4 AL (left-hand side). (B) The same location as (A), taken at ≈ 200 K. A wide stripeless domain phase appears on the left-hand side of the image. (C) Magnification of the rectangle in (A). (D) A high counts image of the stripeless phase at 200 K. (E) Its Fourier power spectrum. (F) Fourier power spectrum of the “stripeless” domain phase of Ref. [13].

already observed [6–8,12]. Simultaneously, more defects appear, as rendered evident by zooming in the rectangular region indicated in Fig. 3A and reproduced in Fig. 3C. Here, stripes are still present, but they follow more tortuous paths. The result is a strong perturbation of the local orientational order. This region of stripes with enhanced local disorder is followed on the left-hand side by a very narrow region where some magnetic contrast is still visible, but one cannot assign it to the formation of well-defined stripes. Further on, the system enters into the paramagnetic region. In order to enlarge the region containing the “stripeless” phase, we have lowered the temperature of the wedge, so that the magnetically active window is considerably enlarged (compare Fig. 3A to 3B). Accordingly, the stripeless phase which was confined to a narrow region in Figs. 3A and 3C occupies a sizable portion of this window; see the left-hand side of Fig. 3B. In order to investigate the stripeless phase in details, we have taken a high resolution image of the region on the left-hand side of Fig. 3B. This image is reported in Fig. 3D. This image reveals that the stripes have indeed broken to pieces, mostly terminating with 90° corners. Two types of corners dominate the image: those with walls along two equivalent $[010]$ directions and those with walls along two equivalent $[110]$ directions of the fcc lattice. Some amount of 45° and 135° corners is also present. The Fourier power spectrum of this image (Fig. 3E) reveals that the stripe phase has lost its strong local orientational order (compare Fig. 3E to Fig. 1D). However, the resulting “liquid” is not isotropic: some tetragonal symmetry remains, reflecting the 90° corners dominating in this phase; see the square shape of the Fourier power spectrum (Fig. 3E). Thus, the stripe phase has orientationally melted into a different phase, which we are tentatively identifying with the “tetragonal liquid crystal” proposed to divide the floating solid from the completely disordered (in our terminology “paramagnetic”) phase [12]. Support for this assignment comes from Monte Carlo simulations [13]. The authors of Ref. [13] produce snapshots of the stripe phase as a function of the temperature. Figure 1d of their paper, which follows the stripe phase before the system completely disorders, shows a picture which resembles our Fig. 3D, except that only corners with walls along $[110]$ are present. Correspondingly, the Fourier power spectrum of their image (Fig. 3F in our paper) displays orientational melting with tetragonal symmetry, the resulting square-shaped Fourier power spectrum reflecting the presence of only one type of corners.

In Ref. [12], the possibility of the existence of a further phase between stripe phase and tetragonal liquid was suggested. This phase is characterized by a type of topological defect called “rotational domain walls.” We do not have enough evidence to identify the region containing stripes with enhanced orientational disorder (Fig. 3C) with the extra phase proposed in Ref. [12], but we cannot exclude that the temperature region in which this extra phase exists is too small to be detected in our images.

The characteristic time for taking the images was not less than 5 min so that the observed fluctuations must have been pinned over such long time scales. We do not know where the pinning comes from: we point out that the Fe/Cu(100) system certainly contains defects on an atomic scale, such as monatomic steps occurring typically every 10 nm [1819]. Pinning is essential: the floating phase as well as the following ones are positionally disordered [10], so that without an efficient pinning on the time scale of the present experiment the images would be completely washed out. Pinning might even alter the temperature dependence considerably: upon cooling, (compare Fig. 3B to 3A) the width of the stripes in the central region did not increase as expected for a truly thermodynamical equilibrium process [12].

At present, we do not know how the paramagnetic phase following the tetragonal liquid phase looks. We cannot exclude that, similarly to the Abrikosov vortex lattice in high T_c superconductors [22], the observed tetragonal liquid phase depins before magnetism is finally lost. In this case, the tetragonal liquid phase would become dynamical, giving rise to a “grey” region of zero polarization where mesoscopic domains exist that fluctuate on a time scale smaller than the time scale of these measurements. In addition, the spatial resolution achieved in the present experiment is at best 20 nm: part of the zero polarization zone could consist, in fact, of domains of smaller scale and go undetected.

A further question one needs to answer is whether the presence of boundaries affects the stripe phase. We have tried to answer this question by imaging the stripe phase in ultrathin films that were grown with limited lateral size [15]. Our results—some of which were already published in Ref. [15]—show that neither the width nor the orientation of the stripes are affected by the presence of boundaries as close as $\approx 1 \mu\text{m}$. Furthermore, ultrathin films with reduced lateral size still show the kind of topological defects that were recorded in extended films (to be published).

There is a number of important issues which are still open. Although we have presented images of a two-step melting process, we were not able to determine the thermodynamical nature of the transitions. This requires measuring some suitable, space integrated thermodynamic quantities and is beyond the capability of our present imaging technique. In addition, one important limitation of SEMPA is that it does not work in the presence of even minute magnetic fields. As the novel feature was expected in zero field exactly, this limitation might have been very important for revealing the novel intermediate phase. On the other side, the phase diagram of the stripe phase offers some interesting challenges when a magnetic field is

applied, either perpendicularly to or inside the film plane [12]. In particular, the phase diagram of the monolayer [12] is predicted to be very different from the one of thick films [2,3]. Finally, the original work by Nelson and Halperin already suggested that the exact symmetry of the substrate (e.g., triangular versus square substrate) plays an important role in the melting process (see also the recent work in Ref. [23]). This important issue, which implies the search for the stripe phase in ultrathin films with suitable symmetry, remains to be explored.

We thank the Swiss National Science Foundation for some financial support. This work was mainly supported by ETH Zurich through a special grant. P.P. acknowledges financial support from the Alexander von Humboldt Stiftung. We thank Professor R. F. Willis for helpful suggestions and C. H. Back for carefully reading the manuscript.

-
- [1] C. Kooy and U. Enz, Philips Res. Rep. **15**, 7 (1960).
 - [2] T. Garel and S. Doniach, Phys. Rev. B **26**, 325 (1982).
 - [3] P. Molho *et al.*, J. Appl. Phys. **61**, 4188 (1987).
 - [4] M. Seul and R. Wolfe, Phys. Rev. Lett. **68**, 2460 (1992), and references therein.
 - [5] Y. Yafet and E. M. Gyorgy, Phys. Rev. B **38**, 9145 (1988).
 - [6] R. Czech and J. Villain, J. Phys. Condens. Matter **1**, 619 (1989).
 - [7] B. Kaplan and G. A. Gehring, J. Magn. Magn. Mater. **128**, 111 (1993).
 - [8] R. Allenspach and A. Bischof, Phys. Rev. Lett. **69**, 3385 (1992); for an extended review, see R. Allenspach, J. Magn. Magn. Mater. **129**, 160 (1994).
 - [9] B. Jancovici, Phys. Rev. Lett. **19**, 20 (1967).
 - [10] N. D. Mermin, Phys. Rev. **176**, 250 (1968).
 - [11] D. R. Nelson and B. L. Halperin, Phys. Rev. B **19**, 2457 (1979).
 - [12] Ar. Abanov, V. Kalatsky, V. L. Pokrovsky, and W. M. Saslow, Phys. Rev. B **51**, 1023 (1995).
 - [13] I. Booth, A. B. MacIsaac, J. P. Whitehead, and K. De’Bell, Phys. Rev. Lett. **75**, 950 (1995).
 - [14] H. D. Sikes and D. K. Schwartz, Science **278**, 1604 (1997), and references therein.
 - [15] C. Stamm *et al.*, Science **282**, 449 (1998).
 - [16] M. Stambanoni *et al.*, J. Appl. Phys. **64**, 5312 (1988).
 - [17] J. Thomassen *et al.*, Phys. Rev. Lett. **69**, 3831 (1992).
 - [18] J. Giergiel *et al.*, Phys. Rev. B **52**, 8528 (1995).
 - [19] U. Ramsperger *et al.*, Phys. Rev. B **53**, 8001 (1996).
 - [20] M. Kosterlitz and D. J. Thouless, J. Phys. C **6**, 1181 (1973).
 - [21] C. H. Back *et al.*, Phys. Rev. B **52**, R13 114 (1995).
 - [22] D. J. Bishop, P. L. Gammel, D. A. Huse, and C. A. Murray, Science **255**, 165 (1992).
 - [23] E. Y. Vedmedenko, A. Ghazali, and J. S. C. Levy, Surf. Sci. **402**, 391 (1998).